Electrodeposition of Nanostructured Films Using Self-Organizing Templates

by Philip N. Bartlett

Over the last 8 years, together with colleagues in Southampton, we have been interested in the templated electrodeposition of regularly structured nanoporous materials and their properties and applications. Over this time we have worked extensively with two different types of self-organizing template: lyotropic liquid crystalline phases and close-packed arrays of spherical colloidal polystyrene particles. The lyotropic liquid crystalline phases produce materials with regular arrays of pores in the 2-10 nm size range with typical wall thicknesses of the same order. The colloidal templates produce materials with close-packed arrays of interconnected spherical pores with diameters that can be varied from around 20 nm to over 1 μm. These nanoporous films may have unique properties which arise either because of the very high surface to volume ratio of the materials, as in materials with the smallest feature sizes templated using lyotropic liquid crystalline phases, or through matching of the dimensions of the structure to some characteristic physical length, as in material produced using colloidal templates.

The idea of templated electrodeposition is not new[1] and has been described by Martin who was the first person to use track-etch membranes to template the deposition of conducting polymer nanowires.[2] Track etch membranes, produced by etching out heavy ion irradiation tracks through a homogeneous membrane, are characterized by a sparse array of uniform diameter pores running approximately perpendicular through the membrane. Martin recognized that these membranes could be used to template the electrochemical deposition of various materials by coating one side of the membrane with an evaporated gold layer and then using this as an electrode for the growth of material through the membrane within the pores. The diameter of the resulting nanorods is controlled by the pore diameter. Subsequent to Martin's work other groups have used this method to produce a range of nanowires and have extended the method to use other membrane templates, notably aluminum oxide membranes formed by anodizing aluminum under controlled conditions.[3]

Our work differs from the studies of deposition of nanowires in that we prepare systems in which the material contains a regular array of nanopores. Nevertheless the same philosophical question arises[2]: how does the presence of the array of nanopores affect the physical properties of the material and to what extent does the imposed nanoporous structure control the properties of the film?

2 to 10 nm: Lyotropic Liquid Crystalline Templates

To prepare the smallest structures we use lyotropic liquid crystalline phases as the templates. These phases are formed by mixing together high concentrations of surfactant and water and have well-defined and characterized structures which depend on the temperature and composition of the mixture.[4] Figure 1 shows a phase diagram for octaethyleneglycol monohexadecyl ether ($C_{16}EO_8$) a nonionic surfactant of the type that we have used widely. The molecule has a hydrophobic 16 carbon alkyl chain with a hydrophilic headgroup comprised of eight ethylene oxide groups, hence the designation $C_{16}EO_8$. At low concentrations in water the mol-

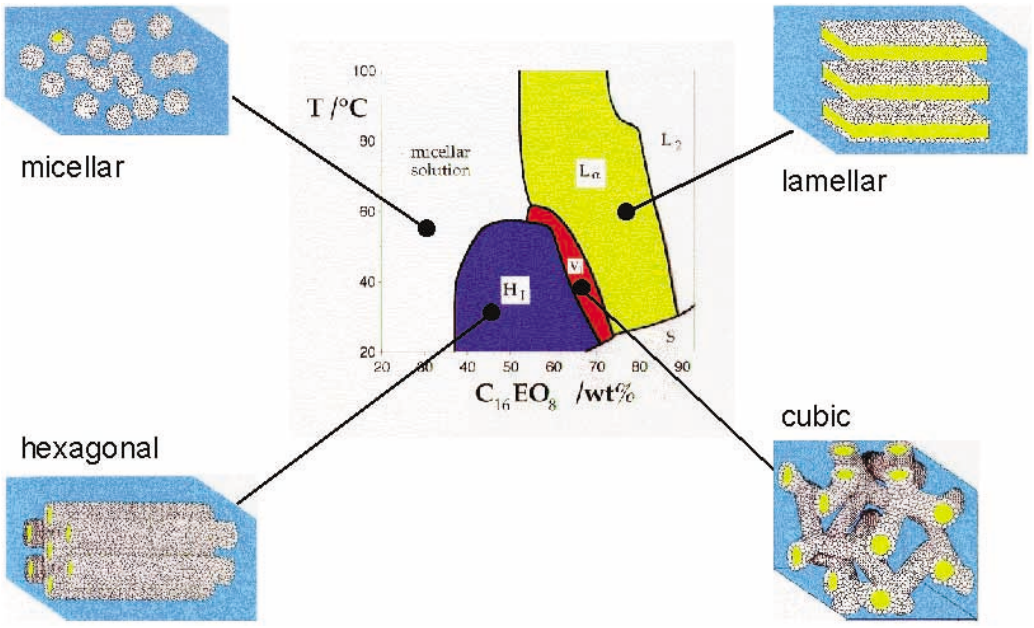

Fig. 1. Phase diagram for the $C_{16}EO_8$/water system showing the micellar structures formed in the different phases (the phase diagram is based on the work of Mitchell et al.[4]*). In the cartoons of the structures, blue represents the water domain, the white circles the hydrophobic ethylene oxide head groups, and the yellow regions the hydrophobic alkyl chains.*

ecules form spherical micelles with the hydrophobic alkyl chains on the inside and the hydrophilic ethylene oxide groups in contact with water on the outside. On increasing the concentration of the surfactant these spherical micelles give way to long cylindrical micelles which pack in hexagonal arrays to give the H_1 hexagonal phase. At still higher concentrations the hexagonal phase gives way to a V_1 bicontinuous cubic phase in which there are two intertwined micellar structures and then at higher concentration still an L_α lamellar phase is formed. The typical dimensions of the structures in these phases are determined by the size of the surfactant molecules which make up the structures and in this case is of the order of 2.5 nm. To use these phases as templates we dissolved the appropriate metal salt and electrolyte in the aqueous domain of the mixture. This can lead to changes in the locations of the boundaries between phases[5] but generally it does not significantly disturb the phase behavior of the system; the same lyotropic phases are formed. When electrodeposition is carried out from the lyotropic phase, the metal is deposited from the aqueous domain and occurs around the surfactant micelles, Fig. 2. Following deposition the surfactant may be removed by washing in water or a suitable solvent to leave a porous metal film with a structure which reflects that of the aqueous domain of the lyotropic liquid crystalline phase.[6] This approach is highly versatile and allows significant control over the size and topology of the pores. For example, by changing between the H_1 hexagonal and V_1 cubic phases it is possible to deposit films with the corresponding templated structures. To date most studies have concentrated on the use of the H_1 hexagonal phase. By changing the surfactant, for example, using $C_{12}EO_8$ rather than $C_{16}EO_8$, or by adding a cosolvent such as *n*-heptane which is immiscible with water, it is possible to systematically vary the diameter of the pores within the metal.[6] The method can be applied to a wide range of materials which can be electrodeposited from aqueous solutions including metals,[6-10] metal oxides,[11] semimetals,[12] polymers,[13] and bimetallic layered structures.[14] To extend this method to produce films with larger pores it is possible to use block copolymer surfactants such as members of the pluronic family (which have the general formula $PO_xEO_yPO_x$, where PO represents hydrophobic propylene oxide units). These systems form similar phases when used as ternary systems with water and an organic solvent such as xylene but with larger structures determined by the size of the polymeric surfactant. However, as yet, templated deposition from these systems has not been explored in any great detail.

Films electrodeposited from lyotropic liquid crystalline phases have high surface areas and contain regular arrays of uniformly sized pores separated by thin walls. These pores run continuously through the films so that, as the film thickness increases, the surface area of the films also increase. This makes them of interest for various applications including uses in batteries and energy storage,[8,15,16] in electrocatalysis,[17,18] electroanalysis,[19] and sensors.[20] The specific surface areas of these films (in cm^2 cm^{-3}) are comparable to those of nanoparticles of similar dimension. Thus for materials deposited from the H_1 phase formed by $C_{16}EO_8$ the calculated specific surface area is 4.7×10^6 cm^2 cm^{-3}, only five times less than that calculated for 2.5 nm diameter nanoparticles. However there are some crucial differences. For many applications of nanopar-

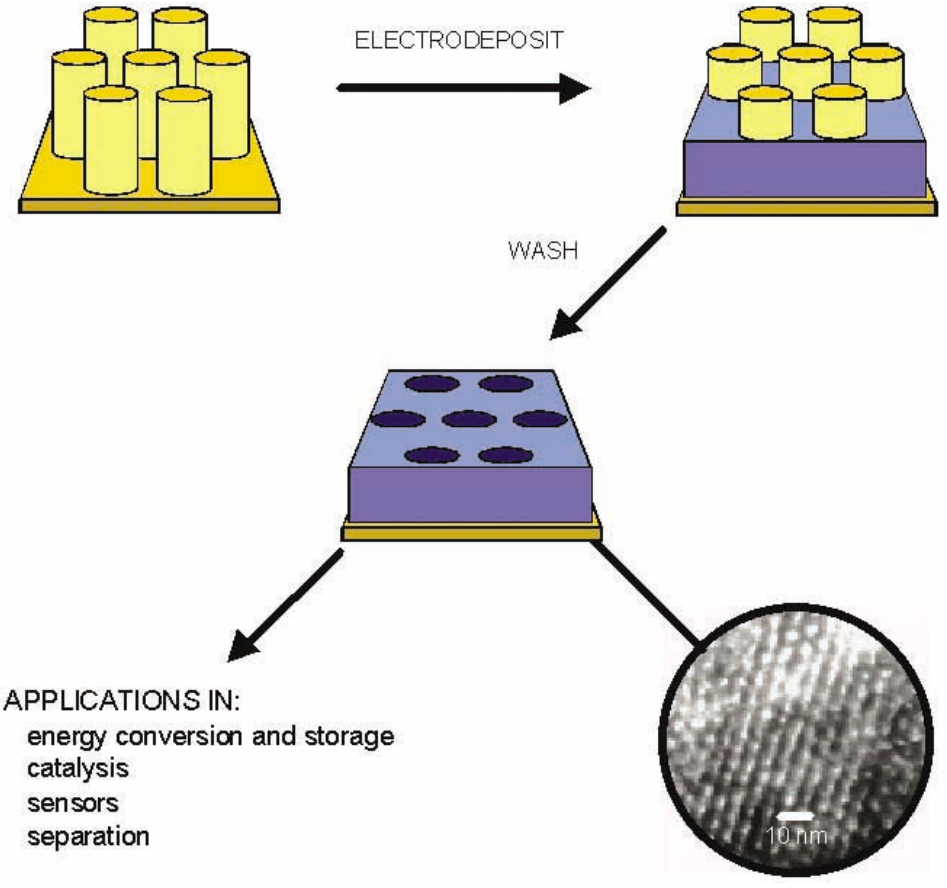

FIG. 2. The principle of the lyotropic liquid crystal templating process illustrated for the H_1 hexagonal phase. The process starts with the plating mixture in the lyotropic liquid crystalline phase. Electrodeposition occurs from the aqueous domain of the phase out from the electrode around the surfactant micelles (represented by the yellow cylinders). Following deposition, the surfactant is removed by washing to leave the nanoporous film whose structure is determined by the structure of the original lyotropic liquid crystalline template. A portion of a TEM image of a Pt film electrodeposited from the H_1 phase of $C_{16}EO_8$ is shown within the circular panel.

ticles it is necessary to provide some suitable conducting support or to agglomerate the particles to allow charge transport through the system from particle to particle. This introduces an interparticle resistance to charge transport through the structure which may limit the charge/discharge rate and hence the power density in devices such as supercapacitors. In contrast the template deposited films are monolithic structures with facile charge transport through the walls of the material and a uniform array of pores which allow rapid ionic transport into the structure. Consequently they show low resistances making them attractive structures for devices where rapid charge or discharge is required.[15]

There is increasing interest in the possible effects of particle size on the efficiency of electrocatalysis. This interest is based on the realization that, as metallic particles approach nanometer dimensions, the surfaces become faceted and the electronic properties of the particles change, both features which can affect the electrocatalytic activity. In contrast to high surface area nanoparticle catalyst surfaces, high surface area films prepared by lyotropic liquid crystalline templating have convex rather than concave surfaces; on average the coordination of atoms in the surfaces of these films is higher than that on the planar surface whereas for the nanoparticles it is lower. This raises the interesting possibility that the catalytic and electrochemical properties of these surfaces may show different behavior because of the difference in curvature, or that the high surface area structures may be kinetically more stable and therefore less susceptible to loss of activity with time.

Examples of applications of films deposited from lyotropic liquid crystalline phases have been reported in the literature. For instance, we have shown that electrodeposition of palladium from the H_1 phase may be used to prepare high surface area catalytic films for gas sensor applications.[20] In this work the palladium was electroplated onto a photolithographically defined gold electrode placed in the center of a micromachined silicon hot plate structure. On heating the hot plate to around 500°C in air, the palladium was converted to a high surface area palladium oxide film which may be used to sense the presence of combustible gases such as methane. The combustible gas reacted with oxygen from the air on the heated catalyst surface changing the temperature of the hot plate and this was sensed by the change in resistance of a platinum track embedded within the microfabricated structure. This application exploits the ability of electrodeposition to control the location and thickness of the catalyst layer together with the use of the templating technique to produce a high surface area active catalytic film. Other applications reported in the literature include studies of these films as electrocatalysts for methanol fuel cells[17,18] and for the direct oxidation of glucose[21] as well as their use in analytical applications as coatings on microelectrodes for oxygen[22] or hydrogen peroxide measurement.[19] An example which illustrates the high ratio of surface area to volume within the films comes from our studies of H_1-e Pd (the notation H_1-e denotes the structure of the material obtained by electrodeposition from the H_1 hexagonal phase).[10,23] For these nanostructured Pd films we find that in the voltammetry in acid we can readily resolve the redox processes corresponding to the formation or stripping of adsorbed hydrogen on the Pd surface and from the formation of the α- and β-hydride phases which, in turn, are well resolved and separate from the onset of hydrogen evolution. For bulk Pd electrodes these different processes are not resolved. The key difference is that the surface area of the H_1-e Pd is very high and the Pd walls within the structure are sufficiently thin

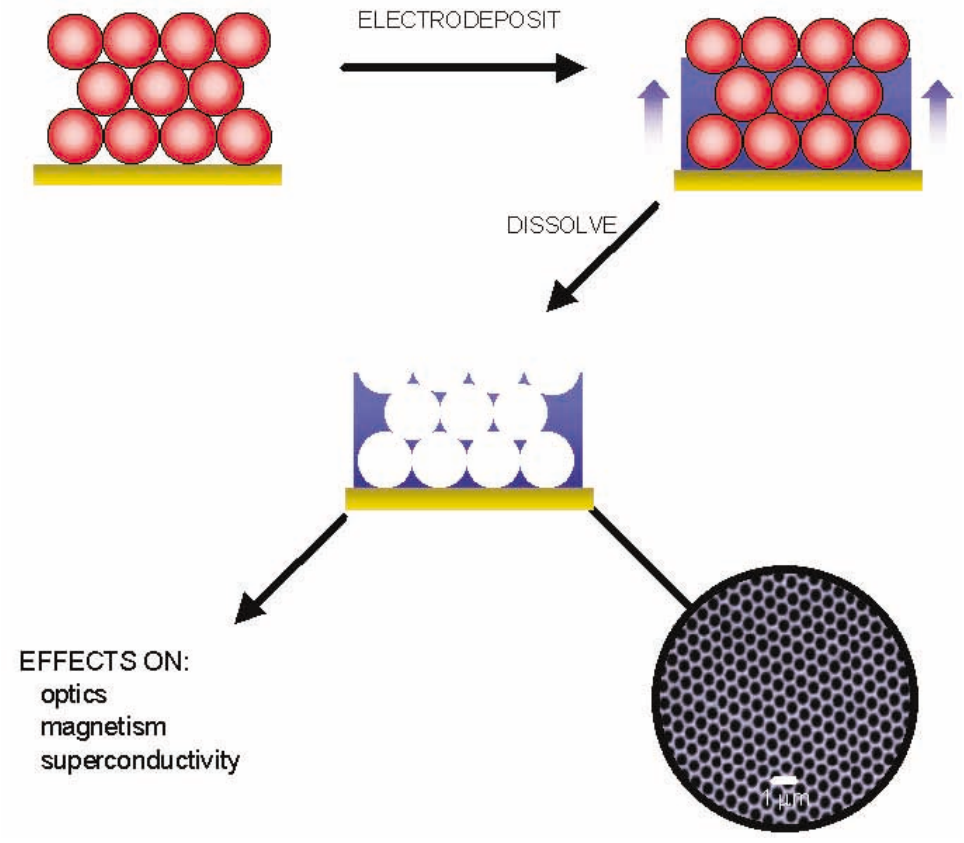

FIG. 3. The principle of colloidal crystal templating. The process starts with the close-packed template of spherical polystyrene particles (red circles) on the electrode surface in contact with the plating mixture. Electrodeposition occurs from the solution out from the electrode surface around the template. Following deposition the template is removed by dissolving the polystyrene in a solvent to leave the macroporous film whose structure is determined by the original template. A portion of an SEM image of a Ni film electrodeposited around a colloidal crystal template is shown within the circular panel.

(around 2.5 nm) that diffusion of hydrogen atoms through the Pd to form the hydride is not rate limiting. We find that when the adsorption of hydrogen on the Pd surface is blocked by adsorption of a poison such as crystal violet or by deposition of a submonolayer coverage of Pt the rate of formation of the β-hydride phase is limited by iR drop in the 1 M sulfuric acid solution.[23]

20 to 1000 nm: Colloidal Crystalline Templates

Spherical colloidal particles with very uniform sizes are commercially available in a range of diameters from around 20 nm to over 1 μm. These particles can be assembled as colloidal crystalline layers on conducting surfaces by various methods such as centrifugation, sedimentation, or evaporation. With careful control of the conditions, it is possible to deposit high quality single crystalline templates over large (>1 mm^2 areas).[24] The assemblies of spheres show striking colors ranging from red to blue depending on the viewing angle due to the effects of Bragg diffraction. This opalescence is identical to that seen for the natural opal gem stone (natural opals are made up of a close-packed array of uniform silica spheres) and is closely related to similar optical effects which give structural color to the plumage of some birds and the wings of several varieties of butterfly.[24]

Much interest in using colloidal crystals to template the formation of materials, particularly semiconductors and oxides, has come from interest in photonic bandgap structures and most materials have been made by infiltration of the colloidal crystal structure with precursors followed by chemical conversion to the desired material and subsequent removal of the template.[25] This leaves an inverse opal structure where there is a close-packed array of regular spherical voids within the material. It is possible to completely remove the template because the spherical voids are interconnected through circular windows which are formed where the spheres of the original template were in contact. A disadvantage of the chemical approach is that there is inevitably shrinkage during conversion of the precursor to the final material (typically by 15% or more). This leads to cracking of the material and it also means that pore size in the final structure is not easily predicted. In addition these chemical methods are not well suited to the fabrication of thin supported macroporous films. Electrodeposition, Fig. 3, overcomes these problems.

The first report of electrodeposition through colloidal templates was in the work of Braun and Wiltzius[26] on the preparation of macroporous CdS and CSe films for photonic bandgap studies. Since that work, some groups including our own have used electrodeposition through colloidal templates to prepare well-ordered inverse opal films of metals and alloys,[27-30] oxides,[31,32] and conducting polymers[33,34] as well as semiconductors. In contrast to chemical approaches, electrodeposition has significant advantages. Electrodeposition ensures a high density of the deposited material within the template voids and leads to volume templating of the structure as opposed to surface templating of material around the template spheres. Consequently there is no shrinkage of the material when the template is removed and no need for further processing steps or the use of elevated temperatures. Hence the resulting macroporous film is a true cast of the template structure and the size of the spherical voids within the film is directly determined by the size of template spheres used. The method is also flexible in the choice of materials which can be used because both aqueous and nonaqueous electrodeposition solutions can be used and the templates are compatible with a wide range of deposition conditions. We have used polystyrene templates in all our work because these templates may be easily removed by soaking in tetrahydrofuran. Silica templates also may be used if polystyrene is unsuitable; in this case the template can be removed by etching in dilute HF.

A unique feature of electrodeposition is that it allows fine control over the thickness of the resulting macroporous film through control over the charge passed. Electrodeposition is thus ideal for the production of thin supported layers for applications such as photonic mirrors since the surface of the film can be uniform.

These nanostructured films are examples of metamaterials, that is, materials whose properties depend on the nature and the particular nanoscale structure of the material. Our primary interest, in collaboration with colleagues in the School of Physics and Astronomy in Southampton, has been to study the effects of the regular macroporous structure on the physical properties and in particular to investigate how these properties change as we systematically vary the diameter of the template spheres and the thickness of the films. The size regime where the feature size matches the natural length scale for the physical property (the wavelength of light, the width of the magnetic domain wall, or the superconducting coherence length) is of particular interest.

Electrodeposited macroporous metal films behave as photonic mirrors; their optical reflectivity depends on the choice of metal, the diameter of the template, and the thickness of the film in a way that is not, as yet, fully understood. Our systematic studies of the effects of angle of incidence, film thickness, and template diameter for Pt, Au, and Ag films show that there are at least three processes which contribute and interact.[35] First, the structures act as sixfold diffraction gratings based on the long-range order of the template.[29] Second, there are interference effects which arise between light reflected from the top surface of the film and light which has undergone one or more reflections within the segment sphere cavities within the film. Finally, for metals such as Au for suitable geometries and angles of incidence we find evidence for the existence of confined surface plasmons within the segment spherical cavities.[36] Our understanding of these effects is still developing but clearly the ability to control the optical properties of these films through control over their geometry on the scale of the wavelength of light offers possibilities for future practical applications in devices.

In the area of magnetism we have investigated the effects of the diameter of the pores and the thickness of porous films on the magnetic properties for Co and NiFe alloy films.[30,37] We find that, as the diameter of the pores decreases, while keeping the thickness of the films constant, the coercivity of the films increases significantly (by a factor of 50 or more). The coercivity is a measure of how easily the direction of magnetization can be switched: hard magnetic materials have large coercivities. For our samples, the increase in coercivity is controlled by domain wall pinning and the magnetic moments rotate out of the plane of the film (Bloch walls).[38] In effect the presence of the spherical voids within the films makes a harder magnetic material by resisting the rotation of the magnetic moments in response to the applied external field. However this effect continues only up to a point. When the pores become very small the coercivity decreases with pore size. The changeover in behavior between these two regimes occurs when the dimensions of the pores are twice the domain wall thickness for the material. For Co this occurs at around 32 nm whereas for 500 nm thick NiFe alloy samples this occurs at about 128 nm.[38] We also find an

intriguing oscillation in the magnetic properties as we increase the film thickness for a fixed pore diameter such that the coercive field passes through a maximum each time the film thickness is such that the top surface of the film is close to the center of a layer of close-packed spherical voids. This oscillation in magnetic properties with film thickness resembles that found for multilayers with alternating hard and soft magnetic layers and constitutes a new class of geometrical multilayer structures.[39]

Nanostructuring films on this scale also affects the superconducting properties of the material. Using Pb films grown through colloidal templates we have investigated the effect of the pore size on superconductivity.[40] Pb is a type I superconductor with a critical temperature of 7.2 K. Below 7.2 K the metal becomes superconducting and, when placed in a external magnetic field, excludes the field up to some critical field which depends on the temperature (this is the Meisner effect). The introduction of defects into the structure (the array of pores defined by the colloidal template) changes the film from a type I to a type II superconductor. In a type II superconductor at temperatures below, but close to, the critical temperature the field lines of an externally applied magnetic field are able to penetrate the sample but the flux is quantized (a fluxon) and a superconducting current is induced around each flux line. This is the so-called vortex state and the presence of these vortices within the superconductor leads to a finite resistance to the passage of current through the sample. For the macroporous samples, the magnetic flux lines are pinned by the regular hexagonal array of nanopores within the film. As a result the resistance of the film in the type II superconducting state shows regular modulations as the strength of the externally applied magnetic field is changed. These oscillations occur when the density of vortices within the film matches the density of pinning sites corresponding to integral numbers of fluxons being associated with each pinning site.[40]

Templating with colloidal particles can be taken one step further in so-called double templated methods. For example, the initial colloidal polystyrene template can be used to template the deposition of a conducting polymer film which, after removal of the polystyrene, can itself be used as a template for the deposition of regular arrays of metal nanodots, Fig. 4. This approach works because the conducting polymer film can be converted to an insulator and because there is a small circular region of the underlying conducting substrate exposed at the bottom of each spherical cavity in the lowest layer of pores in the polymer film. Electrodeposition occurs from each of these conducting regions out through the insulating polymer template. The size and separation of the resulting nanodots is controlled by the size of the initial template spheres and the amount of charge passed in the final electrodeposition step.[41] Similar results have been obtained using nickel oxide as the intermediate template.[42] In a second approach we have used spheres of two different sizes in sequential steps to template the deposition of monolayer arrays of spherical segment pores which are separated from each other. To do this we first assemble the template from the larger spheres and deposit an initial thin layer of metal, less than the radius of the spheres, through this template. We then remove the larger template spheres and replace them with smaller spheres, assembled so that there is one smaller sphere in each cavity templated by the original layer of larger spheres. We then complete the deposition of the film around the smaller spheres and finally remove the smaller spheres to leave an array of pores whose diameter is determined by the size of the smaller spheres and whose spacing is determined by the diameter of the larger spheres.[43]

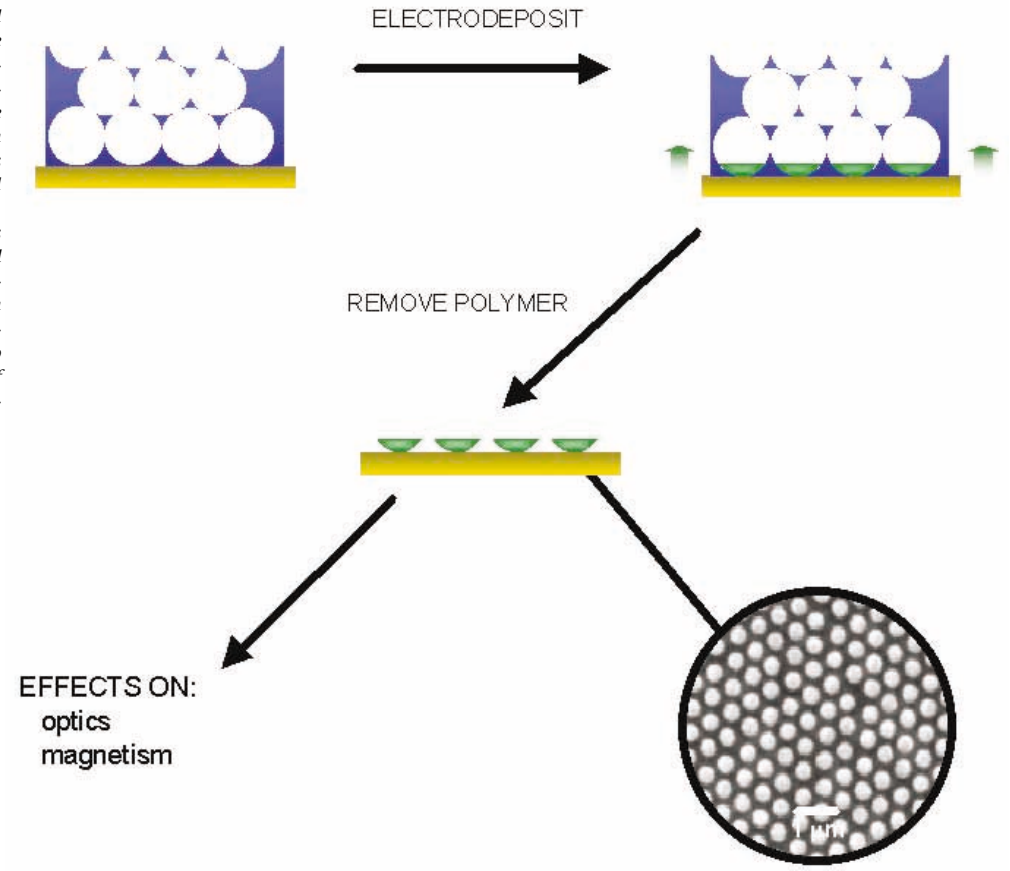

FIG. 4. Principle of the double templated deposition of an array of nanodots. The process starts with a macroporous insulating polymer film (shown in blue) prepared from the colloidal crystal template as shown in Fig. 3. Electrodeposition occurs from the exposed conducting disks at the bottom of each of the spherical pores in the bottom layer of the template. The height of the sphere segments deposited (shown in green) is controlled by the charge passed. Following deposition the polymer is removed to leave an array of nanodots whose spacing is determined by the size of the spheres used to form the original template. A portion of an SEM image of an array of Ni nanodots is shown within the circular panel.

Conclusion

Self-assembled templates allow the electrodeposition of a range of materials containing regular arrays of uniform pores of submicrometer dimension. The presence of these arrays of pores on the hundred nanometer scale alters the physical properties of the material and by varying the size of the pores we can tune the optical, magnetic, and superconducting properties of materials in interesting and possibly useful ways. The presence of arrays of pores on the nanometer scale produces materials with high surface areas and thin pore walls which may find useful applications in energy conversion and storage, electroanalysis, catalysis, and sensors. ■

Acknowledgments

I acknowledge the significant contributions to the work described here made by my colleagues in Southampton in Chemistry (George Attard and John Owen) and in Physics and Astronomy (Peter de Groot and Jeremy Baumberg) and by the students and postdocs working in their research groups and in my own group. Our work has been funded by the Engineering and Physical Sciences Research Council and by City Technology Ltd.

References

1. G. E. Possin, *Rev. Sci. Instrum.,* **41**, 772 (1970).
2. C. R. Martin, *Accounts Chem. Res.,* **28**, 61 (1995).
3. G. Schmid, *J. Mater. Chem.,* **12**, 1231 (2002).
4. D. J. Mitchell, G. J. T. Tiddy, J. Waring, T. Bostock, and M. P. McDonald, *J. Chem. Soc., Faraday Trans. 1,* **79**, 975 (1983).
5. G. S. Attard, P. N. Bartlett, N. R. B. Coleman, J. M. Elliott, and J. R. Owen, *Langmuir*, **14**, 7340 (1998).
6. G. S. Attard, P. N. Bartlett, N. R. B. Coleman, J. M. Elliott, J. R. Owen, and J. H. Wang, *Science*, **278**, 838 (1997).
7. J. M. Elliott, G. S. Attard, P. N. Bartlett, N. R. B. Coleman, D. A. S. Merckel, and J. R. Owen, *Chem. Mater.,* **11**, 3602 (1999).
8. A. H. Whitehead, J. M. Elliott, and J. R. Owen, *J. Power Sources,* **82**, 33 (1999).
9. P. N. Bartlett, P. N. Birkin, M. A. Ghanem, P. de Groot, and M. Sawicki, *J. Electrochem. Soc.,* **148**, C119 (2001).
10. P. N. Bartlett, B. Gollas, S. Guerin, and J. Marwan, *Phys. Chem. Chem. Phys.,* **4**, 3835 (2002).
11. H. M. Luo, J. F. Zhang, and Y. S. Yan, *Chem. Mater.,* **15**, 3769 (2003).
12. I. Nandhakumar, J. M. Elliott, and G. S. Attard, *Chem. Mater.,* **13**, 3840 (2001).
13. J. M. Elliott, L. M. Cabuche, and P. N. Bartlett, *Anal. Chem.,* **73**, 2855 (2001).
14. P. N. Bartlett and J. Marwan, *Chem. Mater.,* **15**, 2962 (2003).
15. P. A. Nelson and J. R. Owen, *J. Electrochem. Soc.*, **150**, A1313 (2003).
16. P. A. Nelson, J. M. Elliott, G. S. Attard, and J. R. Owen, *Chem. Mater.,* **14**, 524 (2002).
17. J. H. Jiang and A. Kucernak, *J. Electroanal. Chem.,* **567**, 123 (2004).
18. A. Kucernak and J. H. Jiang, *Chem. Eng. J.,* **93**, 81 (2003).
19. S. A. G. Evans, J. M. Elliott, L. M. Andrews, P. N. Bartlett, P. J. Doyle, and G. Denuault, *Anal. Chem.,* **74**, 1322 (2002).
20. P. N. Bartlett and S. Guerin, *Anal. Chem.,* **75**, 126 (2003).
21. S. Park, T. D. Chung, and H. C. Kim, *Anal. Chem.,* **75**, 3046 (2003).
22. P. R. Birkin, J. M. Elliott, and Y. E. Watson, *Chem. Commun.,* 1693 (2000).
23. P. N. Bartlett and J. Marwan, *Phys. Chem. Chem. Phys.,* **6**, 2895 (2004).
24. M. Bardosova and R. H. Tredgold, *J. Mater. Chem.,* **12**, 2835 (2002).
25. C. López, *Adv. Mater.,* **15**, 1679 (2003).
26. P. V. Braun and P. Wiltziuz, *Nature*, **402**, 603 (1999).
27. L. Xu, W. L. Zhou, C. Frommen, R. h. Baughman, A. A. Zakhidov, L. M. Malkinski, J.-Q. Wang, and J. B. Wiley, *Chem. Commun.,* 997 (2000).
28. P. N. Bartlett, P. R. Birkin, and M. A. Ghanem, *Chem. Commun.,* 1671 (2000).
29. P. N. Bartlett, J. J. Baumberg, P. R. Birkin, M. A. Ghanem, and M. C. Netti, *Chem. Mater.,* **14**, 2199 (2002).
30. P. N. Bartlett, M. A. Ghanem, I. S. El Hallag, P. de Groot, and A. Zhukov, *J. Mater. Chem.,* **13**, 2596 (2003).
31. P. N. Bartlett, T. Dunford, and M. A. Ghanem, *J. Mater. Chem.,* **12**, 3130 (2002).
32. T. Sumida, Y. Wada, T. Kitamura, and S. Yanagida, *Chem. Lett.,* 38 (2001).
33. T. Sumida, Y. Wada, T. Kitamura, and S. Yanagida, *Chem. Commun.,* 1613 (2000).
34. P. N. Bartlett, P. R. Birkin, M. A. Ghanem, and C. S. Toh, *J. Mater. Chem.,* **11**, 849 (2001).
35. P. N. Bartlett, J. J. Baumberg, S. Coyle, and M. E. Abdelsalam, *Faraday Discuss.,* **125**, 117 (2004).
36. S. Coyle, M. C. Netti, J. J. Baumberg, M. A. Ghanem, P. R. Birkin, P. N. Bartlett, and D. M. Whittaker, *Phys. Rev. Lett.*, art. no. 8717 (2001).
37. A. A. Zhukov, A. V. Goncharov, P. A. J. de Groot, P. N. Bartlett, and M. A. Ghanem, *J. Appl. Phys.*, **93**, 7322 (2003).
38. A. A. Zhukov, A. V. Goncharov, P. A. J. de Groot, P. N. Bartlett, M. A. Ghanem, H. Kupfer, R. J. Pugh, and G. J. Tomka, IEE Proc.-Sci., *Meas., Technol.,* **150**, 257 (2003).
39. A. A. Zuhkov, M. A. Ghanem, A. Goncharov, R. Boardman, V. Novosad, G. Karapetrov, H. Fanghor, P. N. Bartlett, and P. de Groot, *Phys. Rev. Lett.,* Submitted.
40. A. A. Zhukov, E. T. Filby, M. A. Ghanem, P. N. Bartlett, and P. A. J. de Groot, *Physica C,* **404**, 455 (2004).
41. M. A. Ghanem, P. N. Bartlett, P. de Groot, and A. Zhukov, *Electrochem. Commun.,* **6**, 447 (2004).
42. L. Xu, W. Zhou, M. E. Kozlov, I. I. Khayrullin, I. Udod, A. A. Zakhidov, R. H. Baughman, and J. B. Wiley, *J. Am. Chem. Soc.,* **123**, 763 (2001).
43. M. E. Abdelsalam, P. N. Bartlett, J. J. Baumberg, and S. Coyle, *Adv. Mater.,* **16**, 90 (2004).

About the Author

PHIL BARTLETT *is Professor of Electrochemistry at the University of Southampton and Deputy Head of the School of Chemistry responsible for research. He has been involved in electrochemical research for over 25 years and has published more than 175 papers. He is currently a member of the Faraday Council of the Royal Society of Chemistry and a Vice-President of the International Society of Electrochemistry. He may be reached at p.n.bartlett@soton. ac.uk.*